

Strong electron-electron correlation in the antiperovskite compound GaCNi₃

P. Tong, Y. P. Sun,* X. B. Zhu, and W. H. Song

Key Laboratory of Materials Physics, Institute of Solid State Physics, Chinese Academy of Sciences, Hefei 230031, People's Republic of China

(Received 29 December 2005; revised manuscript received 18 May 2006; published 15 June 2006)

We report the structural, magnetic, electrical transport, and specific heat properties of polycrystalline GaCNi₃ sample. The T^2 temperature dependence of resistivity and the large values of the Kadowaki-woods ratio A/γ^2 ($7.2 \mu\Omega \text{ cm}/\text{K}^2$) and the Wilson ratio (9.2) suggest a highly correlated Fermi liquid behavior in GaCNi₃. Such a large electron-electron correlation is due to the proximity of ferromagnetic order from the side of exchange-enhanced Pauli paramagnet, accompanied by remarkable enhancements in the electronic specific heat coefficient γ and the temperature independent magnetic susceptibility χ_0 .

DOI: 10.1103/PhysRevB.73.245106

PACS number(s): 71.27.+a, 75.10.Lp

I. INTRODUCTION

The discovery of superconductivity (the superconducting transition temperature $T_c=8$ K) in antiperovskite compound MgCNi₃ has drawn lots of attentions owing to the high nickel content which may complicate the origin of superconductivity and being a possible link between the traditional intermetallic superconductors and the high T_c oxide ones.¹ It has been theoretically suggested to be an unconventional superconductor and near the instability to the ferromagnetism.² Experimentally, the pairing mechanism of MgCNi₃ is quite controversial. The London penetration depth,³ critical current behavior,⁴ and the earlier tunneling spectra⁵ suggested an unconventional pairing state. While the NMR relaxation rate,⁶ specific heat data,⁷ and the latter tunneling spectra⁸ support a conventional s -wave BCS type behavior. Though no long-range magnetic order has been observed, the FM spin fluctuation has been confirmed to be vigorous in both pristine^{6,7} and doped⁹ MgCNi₃. So far there are many investigations on the doping effects in MgCNi₃. Except for Ni-site doping with Fe, which causes an increase in T_c followed by a decrease with further doping, other doping experiments at either Ni-site,⁹⁻¹² or Mg-site,¹³ or¹⁴ C-site are found to suppress the superconductivity in various ways. In addition, the properties of MgC_{*x*}Ni₃ are very sensitive to the carbon concentration x . The superconductivity disappears when $x \leq 0.88$.¹⁵ The band structure calculation¹⁶ indicates that as x decreases in MgC_{*x*}Ni₃, the proximity to ferromagnetism increases, and the increasing spin fluctuations may be responsible for the reduction of T_c . However the specific heat studies suggest that a lowering of x can reduce the strength of both electron-phonon (e - p) coupling and spin fluctuations and the weakening of e - p coupling would lead to a decrease in T_c .^{17,18} Anyhow the physics of MgCNi₃ is far away from being thoroughly understood at present, therefore more efforts are needed.

Alternatively, the study on the closely related compounds is of interest for pursuing new phenomenon, e.g., superconductivity, as well as for understanding the interplay between superconductivity and ferromagnetism in MgCNi₃. Recently several related nickel-based compounds, i.e., ZnCNi₃,¹⁹ ScB_{0.5}Ni₃,²⁰ and²¹ AlCNi₃ have been synthesized. No superconductivity has been found in either of them. The Zn and Sc

based compounds exhibit Pauli paramagnetic (PM) metallic behavior, while a PM into weak FM transition takes place at near 300 K in AlCNi₃. In this paper we report the synthesis and physical properties of another antiperovskite compound GaCNi₃. A strong electron-electron correlation in this system has been detected through the Kadowaki-Woods ratio and the Wilson ratio. It can be attributable to being on the threshold of ferromagnetism.

II. EXPERIMENTAL DETAILS

The initial ingots of Ga (5N) and powders of Graphite (3N) and Ni (4N) with nominal composition GaCNi₃ were mixed and placed in a molybdenum boat, which was put into a tube furnace and treated at 400°C for 5 h under flowing mixed gas of 95% Ar and 5% H₂. After furnace cooling, the initial mixture became a loose bulk, which was then ground thoroughly and pressed into pellets. Then the pellets were annealed for 10 h at different temperatures varying from 750°C to 850°C to 950°C, respectively under the same atmosphere mentioned above. In order to improve the sample quality, the latter heat treatments were repeated for two more times. No appreciable changes in weight were observed during the heat treatments. With the help of x-ray powder diffraction (XRD) we found that single antiperovskite phase can only be obtained in 950°C sintered pellets. The sample with the size of 1 mm × 3 mm × 5 mm was cut off from a pellet sintered at 950°C for the resistivity measurement, after which the sample was cut into two parts. One was cut into a column shape for magnetic measurements and another into a slice of 0.5 mm × 2.5 mm × 2.5 mm for the specific heat measurement. Our reported data is representative of GaCNi₃ compound annealed at 950°C. X-ray powder diffraction pattern was collected using a Philips X'pert PRO x-ray diffractometer with Cu $K\alpha$ radiation at room temperature. The magnetic, dc resistivity, and specific heat measurements were carried out with a quantum design physical property measurement system (PPMS) ($2 \text{ K} \leq T \leq 400 \text{ K}$, $0 \leq H \leq 90 \text{ kOe}$).

III. RESULT AND DISCUSSION

Figure 1 shows the x-ray diffraction (XRD) pattern of GaCNi₃ annealed at 950°C. As a result of structural refine-

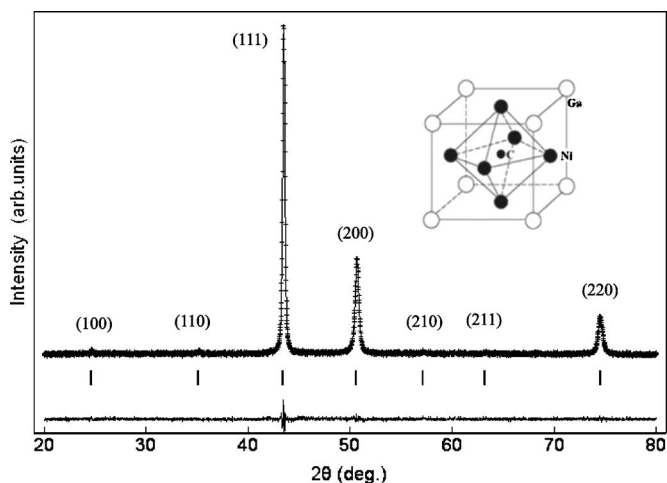


FIG. 1. X-ray diffraction pattern (solid curve) and Rietveld refinement result (crosses) for GaCNi₃ at room temperature. The vertical lines show the Bragg peak positions as denoted by the index (*hkl*). The different plot between the data and the calculation is shown at the bottom. Inset: crystal structure of GaCNi₃.

ment using the standard Rietveld technique, it has single cubic perovskite phase with the space group *Pm3m*, as is found in MgCNi₃.¹ The refined lattice parameter α is 0.3604(5) nm, which is 5% lower than that of MgCNi₃.¹ A distinct feature of its crystal structure is the three dimensional network of CNi₆ octahedron with carbon atoms in the interstitial positions, as shown in the inset of Fig. 1.

Figure 2 depicts the temperature dependence of magnetic susceptibility $\chi(T)$, deduced from the $M(T)$ data measured at an applied field of 1 kOe. For the reason of clarity, only the zero-field cooled (ZFC) curve was plotted since it has no obvious difference with the field cooled (FC) curve. The $\chi(T)$ curve for GaCNi₃ appears to be a PM behavior and can be described by the following expression:²²

$$\chi(T) = \frac{C}{T - \theta} + \chi_0(1 + AT^2). \quad (1)$$

The first term of Eq. (1) stands for the Curie-Weiss contribution to total susceptibility $\chi(T)$. The parameter C , θ ,

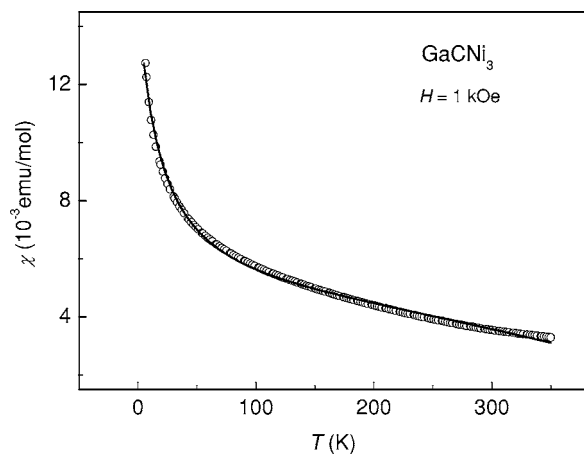


FIG. 2. dc magnetic susceptibility $\chi(T)$ of GaCNi₃ ($H=1$ kOe). The solid line represents the fit to Eq. (1) (see text).

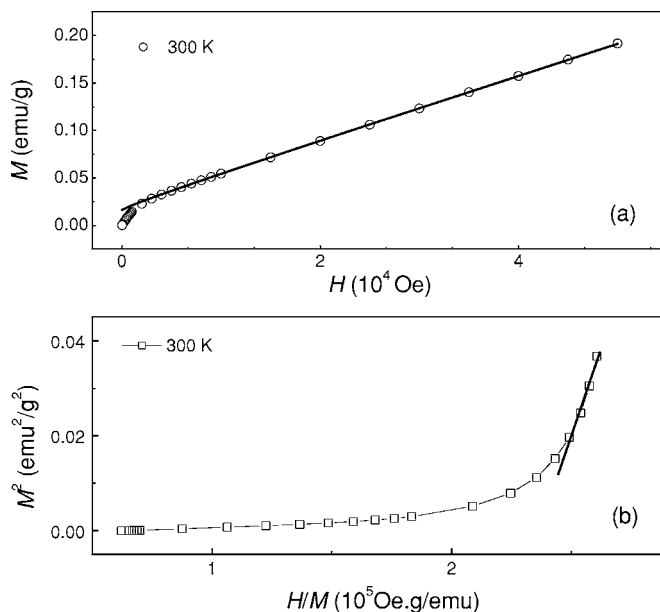


FIG. 3. (a) Magnetization versus magnetic field (M vs H) at 300 K for GaCNi₃; solid line is the linear fitting. (b) Arrott plots (M^2 vs H/M) deduced from (a). Solid line represents the linear extrapolation.

and χ_0 are the Curie constant, PM Curie temperature, and the temperature independent susceptibility, respectively. The fitting result based on Eq. (1) gives the values of parameters, $\chi_0 = 3.9(5) \times 10^{-3}$ emu/mol, $\theta = -19.1(2)$ K, $C = 0.21(6)$ emu K/mol and $A = -2.97(6) \times 10^{-6}$ K, respectively. The effective magnetic moment per Ni atom, μ_{eff} is estimated as $0.75 \mu_B$ from the relationship $\mu_{eff} = 2.83(C/\eta)^{0.5} \mu_B$. Here η is the number of magnetic atoms in a molecular formula and equal to 3 in the present case. The negative value for θ may be a hint of antiferromagnetic (AFM) interaction between the local electrons. It is interesting that the negative θ has often been found in nearly FM or PM systems, while no consistent explanations have been obtained.²²⁻²⁴ In order to subtract the contribution from the possible magnetic impurity the $M(H)$ was measured at 300 K up to 50 kOe. As can be seen in Fig. 3(a), the $M(H)$ exhibits a linear behavior at high magnetic field indicating a PM response to the applied magnetic field. Furthermore in Fig. 3(b), we can see that the extrapolation of high field portion of the Arrott plots to $H/M=0$ yields no positive intercept on the M^2 axis, implying the absence of long range FM ordering. Above 3 kOe, the value of M/H keeps as a constant, 8.4×10^{-4} emu/mol, implying that the magnetization of magnetic impurity if exists is saturated. So in assumption that the contribution resulting from magnetic impurity is temperature independent, the exact value of χ_0 is equal to 3.1×10^{-3} emu/mol after subtraction of the magnetic impurity contribution from the initial one. Ignoring the diamagnetic contribution of core levels and the orbital Van Vleck paramagnetization, the temperature independent susceptibility χ_0 originates from the itinerant electron magnetic susceptibility, which includes both the Pauli PM susceptibility χ_p and the Landau diamagnetic susceptibility χ_d with the expression, $\chi_d = -\frac{1}{3} \left(\frac{m_0}{m^*}\right)^2 \chi_p$, where m^*/m_0 is the enhancement in

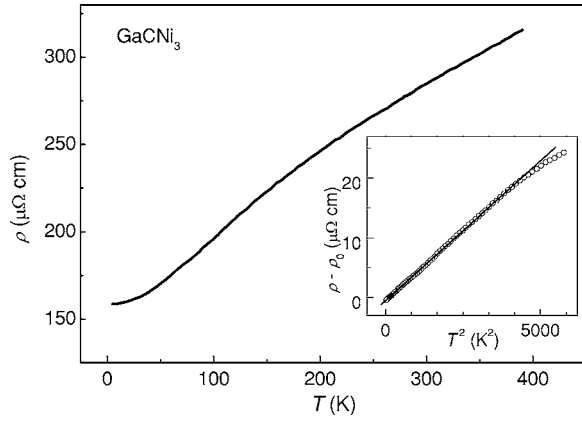


FIG. 4. Temperature dependent resistivity of GaCNi₃. Inset: linear fitting of $\rho(T) - \rho_0$ vs T^2 below 70 K.

effective mass of quasiparticles. According to the analyses of specific heat data in the following text, the value of m^*/m_0 for GaCNi₃ is as large as about 3.3 due to the strong correlated electrons, thus the contribution of Landau diamagnetic susceptibility to χ_0 is negligible, i.e., $\chi_0 \sim \chi_p$. The parameter A reflects the shape of the density of state (DOS) at the Fermi energy E_F .^{22,23}

Figure 4 shows the temperature dependence of the resistivity for GaCNi₃. It exhibits a metallic behavior in the whole temperature range measured and no superconductivity was found down to 2 K. As can be seen in the inset of Fig. 4, below 70 K the resistivity is satisfied with the equation

$$\rho(T) - \rho_0 = AT^2, \quad (2)$$

which is suggestive of a Fermi liquid behavior in the ground state. The residual resistivity ρ_0 and parameter A are found to be 158.5(3) $\mu\Omega$ cm and 0.0046(2) $\mu\Omega$ cm/K², respectively. It is known that the residual resistivity can be written as $\rho_0 \propto m^*/n\tau_0$, where m^* , n , and \hbar/τ_0 represent the effective mass of carriers, mobile carrier concentration, and scattering rate associated with the random potential.²⁵ Since the effective mass m^* for GaCNi₃ is largely enhanced, the large residual resistivity seems to be reasonable. The large residual resistivity of GaCNi₃ is similar to that of polycrystalline SrRhO₃ (142 $\mu\Omega$ cm), which is a strongly enhanced paramagnet close to a magnetic instability with a Wilson ratio of 8.6.²⁶

Figure 5 shows the specific heat for GaCNi₃ measured between 5 and 50 K using a thermal relaxation technique. As shown in the inset of Fig. 5, the data below 18 K, plotted as $C(T)/T$ vs T^2 , can be well fitted using the following formula:

$$C(T)/T = \gamma + \beta T^2 + \delta T^4, \quad (3)$$

where the linear term is the electronic contribution, γ , i.e., the Sommerfeld constant, the second term is the phonon contribution according to the Debye approximation, the last term reflects deviations from the linear dispersion of the acoustic modes in extended temperature range. The fitted values of γ , β , and δ are equal to 25.3(9) mJ/mol K², 0.108(1) mJ/mol K⁴ and $1.3(9) \times 10^{-4}$ mJ/mol K⁶, respectively. By the formula, $\Theta_D = \left(\frac{n \times 1.944 \times 10^6}{\beta}\right)^{1/3}$, where n is the number of atoms in a unit cell, the Debye temperature Θ_D is

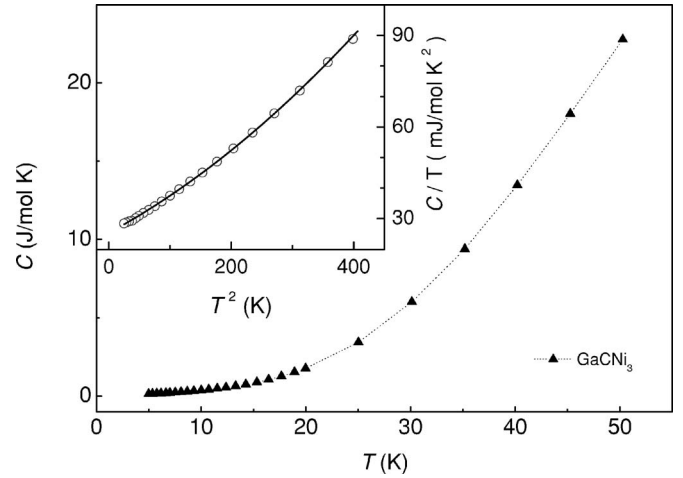


FIG. 5. Specific heat $C(T)$ of GaCNi₃. Inset: $C(T)$ data below 20 K was plotted as $C(T)/T$ vs T^2 (open circles) and fitted using $C(T)/T = \gamma + \beta T^2 + \delta T^4$ (solid line).

448 K, close to that of ZnCNi₃ (421 K), but much larger than that of MgCNi₃ (255.9 K).¹⁹ Comparing the available values of Debye temperature for Ni-based antiperovskite compounds, we can find that the Debye temperature increases with decreasing the lattice parameter a . Namely, the Debye temperature is 255.9, 421, and 448 K for MgCNi₃, ZnCNi₃, and GaCNi₃, corresponding to the lattice parameter a : 0.381, 0.366, and 0.3604 nm, respectively. This behavior may be roughly interpreted as follows: the lattice contract leads to a phonon hardening, correspondingly an increase of Debye temperature.¹⁹ The value of γ for GaCNi₃ is comparable to that of MgCNi₃, 30 mJ/mol K²,¹ but almost 4 times as large as that of ZnCNi₃ (6.77 mJ/mol K²).¹⁹ In MgCNi₃, the large electronic specific heat coefficient is suggested to mainly result from the strong e - p coupling,¹⁷ which supports a superconducting ground state. As will be shown in the following text, the large electronic specific heat coefficient in GaCNi₃ can be ascribed to the strong electron-electron (e - e) coupling. As to ZnCNi₃, the electronic specific heat coefficient is only 6.77(mJ/mol K²), indicating that both the e - e and e - p couplings are weak, in agreement with the Pauli PM ground state.

The Kadowaki-Woods ratio A/γ^2 and the Wilson ratio $R_W = \frac{\pi^2 \kappa_B^2}{3\mu_B^2} \left(\frac{\chi_0}{\gamma}\right)$ are the well-known measures of electron-electron correlation. Here μ_B and κ_B stands for the Bohr magnon and the Boltzmann constant, respectively. Using the values for the coefficient of T^2 in low temperature resistivity, A , the electronic specific heat coefficient (i.e., Sommerfeld constant) γ , and the temperature independent magnetic susceptibility χ_0 , the Kadowaki-Woods ratio A/γ^2 and the Wilson ratio R_W are calculated as 7.2 $\mu\Omega$ cm/K² and 9.2, respectively. The value of A/γ^2 here is on the verge of the universal value of about 10 $\mu\Omega$ cm/K² in the heavy fermion systems,²⁷ suggesting a strongly correlated Fermi liquid behavior in the ground state of GaCNi₃. More markedly, the value of R_W is much larger than unity, which is expected in free electron gas, and well exceeds the strong correlation limit of 2 according to the Anderson model.²⁸ Very large values of R_W have usually been found in the nearly FM ma-

materials due to the Stoner enhancement, such as $\text{Sr}_3\text{Ru}_2\text{O}_7$,²⁴ Pd ,²⁹ and³⁰ TiBe_2 with the value of 10, 6, and 12, respectively.

In order to comprehend the observed behavior, we will refer to the Stoner band theory for itinerant ferromagnetism. Unfortunately, however, as far as we know, no band structure calculation has been performed for GaCNi_3 . Now we attempt to evaluate the density of states (DOS) at the Fermi level (E_F), $N(E_F)$ for GaCNi_3 as follows: The electronic structures of Ni_3Ga and Ni_3Al have been extensively explored as the reference systems for the studies of the itinerant ferromagnetism and exchange-enhanced paramagnetism.³¹ Both of them have the same space group with that of antiperovskite GaCNi_3 and AlCNi_3 , i.e., $Pm\bar{3}m$, while no interstitial C atoms in the body-centered positions. The total $N(E_F)$ for AlCNi_3 , 2.61 states/(eV unit),³² is reduced by 53% when compared with that of Ni_3Al , 5.52 states/(eV unit),³³ due to the hybridization between C-2*p* and Ni-3*d* states. Assuming the same ratio is also available for Ga-based compounds because of the resemblance of these two systems, $N(E_F)$ of GaCNi_3 is estimated to be 1.6 states/(eV spin unit) with the value of 3.4 states/(eV spin unit) for Ni_3Ga .³¹ The feature in the electronic structure of ACNi_3 ($A=\text{Mg, Zn, Al, Ga, et al.}$) is that there exists a DOS peak below the Fermi level, E_F . With increasing the lattice parameter a , regardless of the kind of element A , this peak moves to E_F from the low energy side.³⁴ Correspondingly $N(E_F)$ increases. In this scenario, the $N(E_F)$ of GaCNi_3 should lie between the values of AlCNi_3 and ZnCNi_3 , since its lattice parameter a is larger than AlCNi_3 but less than ZnCNi_3 . So, for GaCNi_3 ,³⁵ $2.61 < N(E_F) < 4.049$ with the unit of states/(eV unit). The above estimated value locates well in this range.

For free electron system without consideration of the correlation between electrons, the Sommerfeld constant γ and Pauli PM susceptibility χ_p can be expected as $\gamma^h = \frac{2}{3}\pi^2\kappa_B^2N(E_F)$ and $\chi_p^h = 2\mu_B^2N(E_F)$. Using 1.6 states/(eV spin unit) as the $N(E_F)$ of GaCNi_3 , γ^h and χ_p^h can be estimated as 7.6 mJ/mol K² and 1.03×10^{-4} emu/mol, respectively. The comparison of the experimental χ_0 with the theoretical χ_p^h leads to a very large Stoner enhancement factor S ($S = \chi_0/\chi_p^h = [1 - IN(E_F)]^{-1}$) of 30.2, where I is the exchange integral that reflects the exchange splitting of the energy bands. The product of $IN(E_F)$, 0.97, is very close to the Stoner criterion $IN(E_F) > 1$ for emergence of long range FM order, implying that GaCNi_3 is in the proximity of the FM order from the exchange-enhanced Pauli PM side. On the other hand, the enhancement of the effective mass for quasiparticles, m^*/m_0 is 3.3, i.e., the ratio of the observed electronic specific heat coefficient γ to that of the expected one γ^h . This effect is related to either e - p coupling or e - e coupling or both. The e - p coupling constant can be estimated by the McMillan's formula,¹⁹

$$\lambda_{ph} = \left[\frac{N(E_F)\langle I^2 \rangle}{M\langle \omega^2 \rangle} \right],$$

where $\langle I^2 \rangle$ is the averaged electron-ion matrix element squared, M is an atomic mass, and $\langle \omega^2 \rangle$ the averaged phonon frequency proportional to Debye temperature Θ_D . For

GaCNi_3 , given that $\langle I^2 \rangle$ and M are the same as in MgCNi_3 , λ_{ph} is evaluated to be 0.24, much less than that of MgCNi_3 , 0.77.¹ Therefore the e - e correlation is the dominant contribution to the observed enhancement in the Sommerfeld constant γ . This result corresponds to the large Stoner enhancement of the temperature independent magnetic susceptibility χ_0 . Moreover, such a strong e - e correlation against a weak e - p correlation, together with the low value of $N(E_F)$, may account for the absence of superconductivity in GaCNi_3 . Now we turn to the relative large value of Wilson ratio in GaCNi_3 . In the self-consistent renormalization (SCR) theory for nearly and weakly itinerant magnets, the Sommerfeld constant γ is suggested to be proportional to $\ln[1 - IN(E_F)]$.³⁶ The increase in $\ln[1 - IN(E_F)]$ is very modest compared with S when $IN(E_F)$ is approaching unity. Consequently, the value of R_W is capable of being larger than 2. Using $IN(E_F) = 0.97$, the ratio (absolute value) of the enhancement in χ_0 to that in γ is about 8.8, which is well consistent with the observed R_W .

To the best of our knowledge, it is possibly the first time to observe such a strong electron-electron correlation in the so-called antiperovskite compounds. Here we note that the electron-electron scattering in GaCNi_3 may be as strong as in the two-layered perovskite $\text{Sr}_3\text{Ru}_2\text{O}_7$ since they have similar A/γ^2 and R_W values.²⁴ Along with the superconductor MgCNi_3 , strongly correlated GaCNi_3 and other related compounds, it is reminiscent of the Ruddleden-Popper (R-P) type ruthenates $(\text{Sr, Ca})_{n+1}\text{Ru}_n\text{O}_{3n+1}$, which have been extensively explored in recent years due to their abundant physical properties. Among them, for instance, Sr_2RuO_4 is a triplet superconductor (for single crystal,³⁷ $T_C = 1.4$ K) connected tightly with the spin fluctuations, i.e., electronic correlation, which has also been discovered in other neighboring compounds, such as FM SrRuO_3 ,³⁸ nearly FM CaRuO_3 ,³⁹ and $\text{Sr}_3\text{Ru}_2\text{O}_7$.²⁴ The ruthenate perovskites and related layered compounds seem to share some similarities with the nickel based antiperovskites ACNi_3 ($A=\text{Mg, Zn, Al, Ga, et al.}$). First, the characteristic structural unit of RuO_6 octahedron, though distorted for some cases can be viewed as the counterpart of CNi_6 octahedron in nickel-based antiperovskites. Second, according to theoretical calculations there exists large hybridization between d and p states in both ruthenate perovskites⁴⁰ and ACNi_3 ,^{2,33} which would account for the itinerant electronic character and heavily influence the low temperature properties.⁴¹ Last, the emergence of vigorous FM correlation in both families probably has some correlations with the superconductivity, i.e., coexistence or competition. In this context, it suggests that studies as to the differences and analogies between these two families would be beneficial to reveal the relationships if it exists between antiperovskites and oxide perovskites, as well as to shed a light on the nature of superconductivity in MgCNi_3 .

IV. CONCLUSION

In summary, the structural, magnetic, electronic transport, and specific heat properties of antiperovskite GaCNi_3 have been investigated. The resistivity exhibits quadratic tempera-

ture dependence below 70 K. The large values of the Kadowaki-woods ratio A/γ^2 and the Wilson ratio R_W indicate a strong electron-electron correlation, being attributed to the instability to FM order. The similarity between the nickel-based antiperovskites, e.g., GaCNi_3 and MgCNi_3 and the R-P type ruthenates, e.g., p -wave superconductor Sr_2RuO_4 and strongly correlated $\text{Sr}_3\text{Ru}_2\text{O}_7$ has also been discussed in brief.

ACKNOWLEDGMENTS

This work is supported by the National Key Basic Research under Contract No. 001CB610604, and the National Nature Science Foundation of China under Contract No. 10474100, and Fundamental Bureau of Chinese Academy of Sciences.

*Corresponding author. Tel.: +86-551-559-1436; fax: +86-551-559-1434. E-mail address: ypsun@issp.ac.cn

- ¹T. He, Q. Huang, A. P. Ramirez, Y. Wang, K. A. Regan, N. Rogado, M. A. Hayward, M. K. Haas, J. S. Slusky, K. Inumara, H. W. Zandbergen, N. P. Ong, and R. J. Cava, *Nature (London)* **411**, 54 (2001).
- ²H. Rosner, R. Weht, M. D. Johannes, W. E. Pickett, and E. Tosatti, *Phys. Rev. Lett.* **88**, 027001 (2002).
- ³R. Prozorov, A. Snezhko, T. He, and R. J. Cava, *Phys. Rev. B* **68**, 180502(R) (2003).
- ⁴D. P. Young, M. Moldovan, and P. W. Adams, *Phys. Rev. B* **70**, 064508 (2004).
- ⁵Z. Q. Mao, M. M. Rosario, K. D. Nelson, K. Wu, I. G. Deac, P. Schiffer, Y. Liu, T. He, K. A. Regan, and R. J. Cava, *Phys. Rev. B* **67**, 094502 (2003).
- ⁶P. M. Singer, T. Imai, T. He, M. A. Hayward, and R. J. Cava, *Phys. Rev. Lett.* **87**, 257601 (2001).
- ⁷L. Shan, Z. Y. Liu, Z. A. Ren, G. C. Che, and H. H. Wen, *Phys. Rev. B* **71**, 144516 (2005).
- ⁸L. Shan, H. J. Tao, H. Gao, Z. Z. Li, Z. A. Ren, G. C. Che, and H. H. Wen, *Phys. Rev. B* **68**, 144510 (2003).
- ⁹T. G. Kumary, J. Janaki, A. Mani, S. M. Jaya, V. S. Sastry, Y. Hariharan, T. S. Radhakrishnan, and M. C. Valsakumar, *Phys. Rev. B* **66**, 064510 (2002).
- ¹⁰M. A. Hayward, M. K. Haas, A. P. Ramirez, T. He, K. A. Regan, N. Rogado, K. Inumaru, and R. J. Cava, *Solid State Commun.* **119**, 491 (2001).
- ¹¹A. Das and R. K. Kremer, *Phys. Rev. B* **68**, 064503 (2003).
- ¹²T. Klimczuk, V. Gupta, G. Lawes, A. P. Ramirez, and R. J. Cava, *Phys. Rev. B* **70**, 094511 (2004).
- ¹³S.-H. Park, Y. W. Lee, J. Giim, Sung-Hoon Jung, H. C. Ri, and E. J. Choi, *Physica C* **400**, 160 (2004).
- ¹⁴T. Klimczuk, M. Avdeev, J. D. Jorgensen, and R. J. Cava, *Phys. Rev. B* **71**, 184512 (2005).
- ¹⁵T. G. Amos, Q. Huang, J. W. Lynn, T. He, and R. J. Cava, *Solid State Commun.* **121**, 73 (2002).
- ¹⁶P. J. Joseph and P. P. Singh, *Phys. Rev. B* **72**, 064519 (2005).
- ¹⁷A. Wälte, G. Fuchs, K.-H. Müller, S.-L. Drechsler, K. Nenkov, and L. Schultz, *Phys. Rev. B* **72**, 100503(R) (2005).
- ¹⁸L. Shan, K. Xia, Z. Y. Liu, H. H. Wen, Z. A. Ren, G. C. Che, and Z. X. Zhao, *Phys. Rev. B* **68**, 024523 (2003).
- ¹⁹M.-S. Park, J. Giim, S.-H. Park, Y. W. Lee, S. I. Lee, and E. J.

- Choi, *Supercond. Sci. Technol.* **17**, 274 (2004).
- ²⁰T. Shishido, K. Kudou, T. Sasaki, S. Okada, J. Ye, K. Iizumi, A. Nomura, T. Sugawara, K. Obara, M. Tanaka, S. Kohiki, Y. Kawazoe, K. Nakajima, and M. Oku, *J. Alloys Compd.* **383**, 294 (2004).
- ²¹A. F. Dong, G. C. Che, W. W. Huang, S. L. Jia, H. Chen, and Z. X. Zhao, *Physica C* **422**, 65 (2005).
- ²²S. N. Kaul, A. Semwal, and H.-E. Schaefer, *Phys. Rev. B* **62**, 13892 (2000).
- ²³I. H. Inoue, O. Goto, H. Makino, N. E. Hussey, and M. Ishikawa, *Phys. Rev. B* **58**, 4372 (1998).
- ²⁴S. I. Ikeda, Y. Maeno, S. Nakatsuji, M. Kosaka, and Y. Uwatoko, *Phys. Rev. B* **62**, R6089 (2000).
- ²⁵G. M. Zhao, D. J. Kang, W. Prellier, M. Rajeswari, H. Keller, T. Venkatesan, and R. L. Greene, *Phys. Rev. B* **63**, 060402(R) (2000).
- ²⁶K. Yamaura and E. Takayama-Muromachi, *Phys. Rev. B* **64**, 224424 (2001).
- ²⁷K. Kadowaki and S. B. Woods, *Solid State Commun.* **58**, 507 (1986).
- ²⁸K. G. Wilson, *Rev. Mod. Phys.* **47**, 773 (1975).
- ²⁹F. M. Mueller, A. J. Freeman, J. O. Dimmock, and A. M. Furdyna, *Phys. Rev. B* **1**, 4617 (1970).
- ³⁰T. Jarlborg and A. J. Freeman, *Phys. Rev. B* **22**, 2332 (1980).
- ³¹A. Aguayo, I. I. Mazin, and D. J. Singh, *Phys. Rev. Lett.* **92**, 147201 (2004).
- ³²A. L. Ivanovskii, *Phys. Solid State* **45**, 1829 (2003).
- ³³I. Hase, *Phys. Rev. B* **70**, 033105 (2004).
- ³⁴C. M. I. Okoye, *Solid State Commun.* **136**, 605 (2005).
- ³⁵M. D. Johannes and W. E. Pickett, *Phys. Rev. B* **70**, 060507(R) (2004).
- ³⁶C. J. Fuller, C. L. Lin, T. Mihalisin, F. Chu, and N. Bykovetz, *J. Appl. Phys.* **73**, 5338 (1993).
- ³⁷K. D. Nelson, Z. Q. Mao, Y. Maeno, and Y. Liu, *Science* **306**, 1151 (2004).
- ³⁸J. Okamoto, T. Mizokawa, A. Fujimori, I. Hase, M. Nohara, H. Takagi, Y. Takeda, and M. Takano, *Phys. Rev. B* **60**, 2281 (1999).
- ³⁹T. He and R. J. Cava, *Phys. Rev. B* **63**, 172403 (2001).
- ⁴⁰T. Oguchi, *Phys. Rev. B* **51**, 1385 (1995).
- ⁴¹G. Cao, S. McCall, M. Shepard, J. E. Crow, and R. P. Guertin, *Phys. Rev. B* **56**, 321 (1997).